LU TP 06-17
April 2006

Fermi-Dirac Correlations Between Protons in the String Fragmentation Picture

Master of Science Thesis by Rosa María Durán Delgado
Thesis advised by Gösta Gustafson and Leif Lönnblad
Department of Theoretical Physics
Lund University, Sweden

Abstract

The Fermi-Dirac correlation between protons produced in hadronic e^+e^--annihilation events has recently been determined at LEP, yielding a value for the source radius that is smaller than the proton radius itself. In this thesis we present a review of the methods used for the derivation of the two-particle correlation, stressing the important role of Monte Carlo simulations of events in the analysis of the experimental data. We discuss how imperfections in the Monte Carlo simulations could be affecting the value of the source radius. The correlation exhibits some dependence on the parameters a and b of the Lund string fragmentation model and on the different baryon production scenarios. The effects studied here are significant, but not large enough to fully explain the unexpected results in experimental analyses. Further studies will be needed to reveal the true nature of the Fermi-Dirac correlation.

LUND UNIVERSITY

Contents

1 Introduction

"I ask you to look both ways. For the road to a knowledge of the stars leads through the atom; and important knowledge of the atom has been reached through the stars."

Sir Arthur Eddington (1882 - 1944). Stars and Atoms (1928), Lecture 1

Consider the emission of two identical bosons from two points lying within a continuous distribution of particle sources, such as a star. Since these particles obey the Bose-Einstein statistics, the amplitude A_{12} for observing the two bosons simultaneously is totally symmetric with respect to the exchange of the bosons. The probability of detecting both particles at the same time, $P_{12} \propto |A_{12}|^2$, will depend, in general, not only on the characteristics of the particle source and the momenta of the particles, but also on the nature of the experiment, i.e. whether it is *coherent*, *chaotic or incoherent*, or *partially chaotic*. In the totally *coherent* case, e.g. in a laser beam, it is not possible to uniquely determine, by any kind of measurement, in which two points of the source distribution the bosons were emitted. In this case, and assuming that the bosons do not interact classically, the probability P_{12} simply equals the product of the probabilities P_1 and P_2 of observing the particles separately [1]. However, if the process includes any degree of incoherence, an enhancement of the probability P_{12} is found whenever the two bosons have similar energy-momenta, a phenomenon commonly referred to as *Hanbury Brown-Twiss (HBT) effect* or *Bose-Einstein (BE) effect*.

It may seem strange that the HBT effect, being of a purely quantum mechanical nature, was first measured in the 1950s, through a technique called intensity interferometry, as a means of determining the dimension of astronomical objects. Hanbury Brown and Twiss developed this technique [2], in which the photons coming from an astronomical object are counted in two different detectors D_1 and D_2. With the number of photons detected at D_1, n_1, the number of photons at D_2, n_2, and the number of photons detected simultaneously at D_1 and D_2, n_{12}, a correlation function C is constructed as:

$$C = \frac{\langle n_{12} \rangle}{\langle n_1 \rangle \langle n_2 \rangle} \propto \frac{P_{12}}{P_1 P_2} = 1 + |\mathcal{R}(q)|^2 \tag{1}$$

The last identity above, which will be derived in the theoretical review of Sect. 2, relates the two-particle correlation function to the size of the distribution of boson sources and their lifetime, given that $\mathcal{R}$ is the normalised Fourier transform of the space-time source density $\rho(x)$:

$$\mathcal{R}(q) = \frac{\int \rho(x) \exp(iqx)\ dx}{\int \rho(x)\ dx} \tag{2}$$

The variable q denotes the difference in the four-momenta of the bosons, $q = p_1 - p_2$ (we set $\hbar = c = 1$) . However, we will hereafter use the more common parameter Q instead, which is defined from $Q^2 = -q^2$, so that Q^2 is a positive Lorentz invariant.

In this framework, Hanbury-Brown and Twiss were able to demonstrate experimentally the BE effect between astronomical photons. It was soon realized that the BE effect may as well apply to particles produced in collisions (annihilations) of elementary particles. In 1959 Goldhaber *et al.* observed, for the first time, a BE enhancement in the production of pions from proton-antiproton collisions close to the threshold [3]. For the analysis of the measured correlations, they developed a parametrisation that assumes a spherically symmetric source volume with a Gaussian density in the rest frame of the emitted pair. The two-particle correlation function is thus parametrised in terms of a "source radius" R, a "chaoticity" parameter λ and a normalization constant $\mathcal{N}$:

$$C = \mathcal{N}[1 + \lambda \exp(-R^2 Q^2)] \tag{3}$$

According to geometrical models, the R parameter can be identified with a source radius [4]. This interpretation may be considered appropriate in the astrophysical HBT application, where it is assumed that the spatial characteristics of the emitter do not change over the time scale of the measurements. Unfortunately this is not true in the case of elementary-particle collisions. Any relativistically covariant theory for multiparticle production, such as the *Lund model*, states that the production regions typically move at relativistic velocities with respect to each other. Hence, in principle the general interpretation of R is not simple.

Following the Goldhabers, a sizable number of experiments were performed in order to measure the BE correlations between pions or kaons produced in different kinds of hadronic interactions. The values obtained for the "source radius" in all the experiments were remarkably similar, in the range $R \sim 0.5 - 1\,fm$.

Recently, the ALEPH, DELPHI and OPAL collaborations have performed correlation measurements for produced $\Lambda\Lambda$, $\bar{\Lambda}\bar{\Lambda}$, protons pp and antiprotons $\bar{p}\bar{p}$, which are baryons, i.e. fermions. The *Fermi-Dirac (FD) effect* is readily defined as a depletion in the probability of non coherent emission of two identical fermions close in energy-momentum, relative to the single particle emission probability, which arises as a consequence of the antisymmetrization of the two-particle wavefunction (Pauli exclusion principle). The Goldhaber parametrisation becomes then for the fermions:

$$C = \mathcal{N}[1 - \lambda \exp(-R^2 Q^2)] \tag{4}$$

The baryon-correlation measurements all come from e^+e^- collisions at the Z^0 mass energy ($\sim 91GeV$). Some 3 to 4 million hadronic Z^0 decays were recorded at the LEP collider by each of the ALEPH, DELPHI and OPAL detectors, so that, finally, enough statistics are available to begin the study of FD correlations, in spite of the low production rate of identical baryons in particle reactions. A summary of the λ and R values derived from the FD correlation analyses is given in Table 1. Surprisingly, the average value for the "source radius" $R \sim 0.15fm$ is not only small as compared to the meson "source radii", it is even smaller than the radii of the proton and Lambda themselves $\sim 0.8fm$!

These results are rather difficult to conciliate with the original HBT theory, with the ideal extensive distribution of sources emitting point-like particles independently. We could assume that R is not associated with the space-time extent of the source distribution. The Lund model, for example, suggests that R determines the region inside which the quantum

	$R\,(fm)$	λ	**Experiment**	
$\Lambda\Lambda$	0.19 ± 0.07	Spin Analysis	OPAL	[5]
	0.11 ± 0.05	Spin Analysis	DELPHI	[6]
	0.17 ± 0.13	Spin Analysis	ALEPH	[7]
	0.11 ± 0.02	0.59 ± 0.09	ALEPH	[7]
$\bar{p}\bar{p}$	0.14 ± 0.04	0.76 ± 0.16	OPAL	[8]
	0.11 ± 0.01	0.49 ± 0.08	ALEPH	[9]
	0.16 ± 0.04	0.67 ± 0.19	DELPHI	[10]

Table 1: Experimental results for λ and R from FD correlations between baryon-pairs produced in e^+e^- annihilations at the LEP collider.

numbers of the production process are compensated, which may explain why the "source size" does not apparently depend upon the kind of interaction or the energies involved in the reactions. However, is it possible to explain the fact that $R_{baryons} < R_{mesons}$ within the framework of this picture? Certainly, this is not an easy task. Another possible approach to the problem would be to assume that a different quantum mechanism, yet not understood, is behind the interactions measured between the particles. But, before that, are we certain about the reliability of the experimental results? Let us first explain the two techniques most commonly used for the analysis of the fermion correlations.

The first method makes use of a reference sample in order to get rid of all the correlations between the identical particles except for their quantum FD interference; for example it should include the correlations derived from the energy-momentum conservation, baryon number conservation, event topology, etc. The correlation function is constructed as:

$$C(Q) = \frac{N(Q)}{N(Q)^{REF}} \tag{5}$$

where $N(Q)$ is the measured differential cross section for the real pairs and $N(Q)^{REF}$ is that for the pairs in the reference sample, which, as we said, should be free of BE and FD correlations but otherwise identical in all aspects to the data sample. Such an ideal reference sample really does not exist, but there are some approximate alternatives that we briefly describe in the following.

- A Monte Carlo (MC) generated sample is very frequently used. PYTHIA, for example, is an event generator based on the Lund string model, which approximately reproduces the dynamics of the hadronization process, but without any BE or FD interference.

- The reference sample can be constructed out of the actual experimental data, by coupling two fermions each originating from a different data event, i.e. from a different collision. This "mixed-event" sample clearly removes all FD effects, but also all other kinds of correlations. Furthermore, at high-energy collisions the particles emerge in several hadron-jets. The mixed event technique can only be reliably applied to two-jet events where the mixing takes place between events with their thrust axes[1] lying in the same direction (the events need to be rotated so that the two event axes coincide). In order to re-include the interactions non-attributed to FD effects and to correct for imperfections, the so called “double ratio” is generally used:

$$C(Q) = \frac{N(Q)}{N(Q)^{mix}} \Bigg/ \frac{MC(Q)}{MC(Q)^{mix}} = \frac{N(Q)}{MC(Q)} \cdot \frac{MC(Q)^{mix}}{N(Q)^{mix}} \tag{6}$$

where $MC(Q)$ represents a MC generated sample and $MC(Q)^{mix}$ a MC mixed event sample. The ratio $MC(Q)^{mix}/N(Q)^{mix}$ is expected to be a slowly varying function w.r.t. Q, ideally flat, which will hence provide only minor corrections to the correlation function $C(Q) = N(Q)/MC(Q)$, i.e. to the correlation function obtained with the MC generated reference sample.

- Another data derived reference sample can be constructed by pairing the particles of interest with oppositely charged particles of the same type produced in the same event. This kind of reference sample was used in many studies of meson correlations, but this choice has rather severe drawbacks. Unlike-sign pairs (opposite charged pairs) may originate from resonances, so that the experimental ratio $N(Q)/N(Q)^{unlike}$ could only be analysed with a fit to (4) in the Q regions where the data is known to be free of resonances. Also, due to the geometry of the hadronization process (see section 3), the unlike-sign pairs have stronger correlations than the real pairs, and thus we need to correct the measured correlations with a double ratio, as for the mixed events. Hence, this reference sample would also yield a correlation very similar to that obtained using a MC generated sample.

The second method for the analysis of FD correlations is referred to as the *spin analysis technique*. This technique has the advantage that it does not need a reference sample, but it also has some bad points, for instance, that it can only be used for spin 1/2 baryons which weakly decay into other hadrons. This is why the technique has been applied to $\Lambda\Lambda$ pairs but not to proton pairs, as we can see in Table 1. The method relies on the fact that as Q approches zero the only possible energy-state is the S ($l = 0$) state (assuming there are no di-baryon resonances); then, according to the Pauli exclusion principle, the total spin of the pair of baryons $\vec{S} = \vec{S_1} + \vec{S_2}$, with eigenvalues $S = \{0, 1\}$, can only acquire the value $S = 0$. Thus, in theory, the system should be a spin mixture ensemble for high values of Q, and gradually become a set of only $S = 0$ states as Q decreases. In the mixture ensemble the spin states which are present are the state s_0 corresponding to $S = 0$, and the three states s_1^i, where $i = \{-1, 0, 1\}$ are the three different eigenvalues of S_z for $S = 1$; all four states are emitted with the same probability. Therefore the $S = 1$ contribution to the correlation function $C(Q)$, denoted by $C(Q)_{S=1}$ hereafter, dominates by a factor of three in the mixture

[1]See definition in section 4.

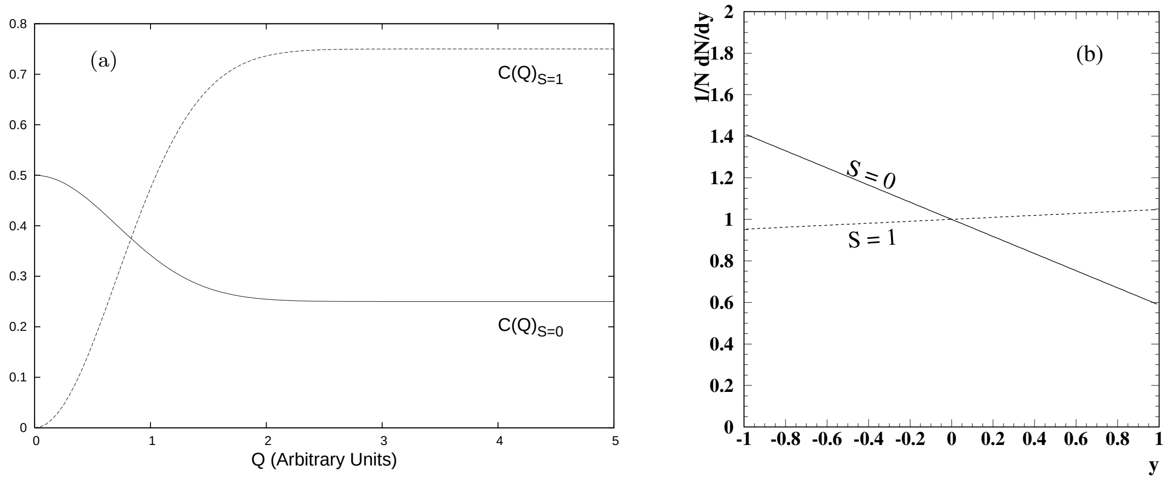

Figure 1: (a) Schematic view of the ideal contributions of the states with total spin $S = 0$ and $S = 1$, of an identical spin 1/2 two-fermion system, to the normalized FD correlation function $C(Q)$. (b) Ideal contributions of the $S = 0$ and $S = 1$ states to the angular distribution of the hadrons, decay products of the original spin 1/2 two-fermion system.

ensemble. The separate contributions, which satisfy $C(Q)_{S=0} + C(Q)_{S=1} = C(Q)$, can be parametrised with the following equations, plotted in Fig. 1 (a):

$$C(Q)_{S=0} = 0.25\mathcal{N}[1 + \exp(-R^2Q^2)] \qquad C(Q)_{S=1} = 0.75\mathcal{N}[1 - \exp(-R^2Q^2)] \tag{7}$$

As explained for example in reference [11] or [7], a measure of the angular distribution of the protons in which the Λs decay can provide us with the value of ϵ, the fraction of the $S = 1$ contribution, $\epsilon = C(Q)_{S=1}/[C(Q)_{S=0} + C(Q)_{S=1}]$. It is clear that this quantity can also be used to estimate the source radius, since from (7) one finds:

$$\epsilon = \frac{0.75[1 - \exp(-R^2Q^2)]}{1 - 0.5\exp(-R^2Q^2)} \tag{8}$$

The chaoticity parameter is normally fixed to the value $\lambda = 0.5$ when using this method (note that the sum of the expressions $C(Q)_{S=0}$ and $C(Q)_{S=1}$ of eq. (7) gives the function $C(Q) = \mathcal{N}[1 - 0.5\exp(-R^2Q^2)]$). For a more realistic situation that accounts for possible resonances and final-state interactions between the pair of particles, a parameter γ is sometimes used in the equations (7), as a coefficient multiplying the exponential terms, so that the quantity $\epsilon(Q)$ becomes $\epsilon = 0.75[1 - \gamma\exp(-R^2Q^2)]\Big/[1 - 0.5\gamma\exp(-R^2Q^2)]$. Another possible variation of eq. (8), suggested by the OPAL Collaboration [5], is to assume that $\epsilon(Q)$ follows a Goldhaber parametrisation $\epsilon = 0.75[1 - \gamma\exp(-R^2Q^2)]$, which would yield a larger value for R. The results for R using all these parametrisations are notwithstanding very similar.

It is probably more interesting to mention how the function $\epsilon(Q)$ is derived. The distribution of the decay protons of the ΛΛ system is measured as a function of y^*, the

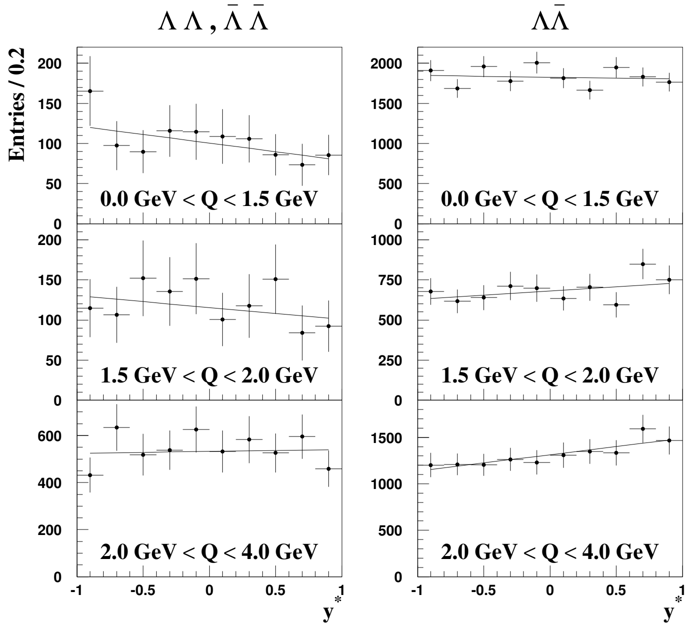

Figure 2: The corrected distributions $dN/dy^*|_{corr}$ obtained for the ($\Lambda\Lambda$) and ($\Lambda\bar{\Lambda}$) data, the latter free from FD correlations, by the ALEPH Collaboration [7].

cosine of the angle between the two protons in the di-hyperon centre-of-mass system. Then, in order to correct for losses due to acceptance effects and for background contributions, the measured angular distribution $dN/dy^*|_{data}$ is multiplied by a factor obtained from Monte Carlo simulations:

$$dN/dy^*|_{corr} = dN/dy^*|_{data} \frac{dN/dy^*|_{MC,generator}}{dN/dy^*|_{MC,with\ detector\ simulation}} \tag{9}$$

If the FD effect is present between the $\Lambda's$ of the pairs, then it is more likely for the decay protons to be emitted at large relative angles, i.e. we would expect an enhancement in $dN/dy^*|_{corr}$ as y^* decreases. The specific angular distributions for pure $S = 0$ and $S = 1$ di-hyperon states, obtained from the so-called Wigner-Eckart theorem, are shown in Fig. 1 (b). The total angular distribution is then given by $dN/dy^*|_{corr} = (1-\epsilon)dN/dy^*|_{S=0} + \epsilon dN/dy^*|_{S=1}$, and thus it is perfectly feasible, in principle, to derive the spin composition $\epsilon(Q)$ from this method. The main disadvantage of the spin analysis technique, however, is its need for a very large data sample. The actual analyses by the OPAL, DELPHI and ALEPH Collaborations have been performed with rather low statistics. As an example, in Fig. 2 we show the data obtained by the ALEPH Collaboration [7]. In the region $0\,GeV < Q < 1.5\,GeV$ we expect to see a gradual decrease for increasing y^* for the $\Lambda\Lambda$ pairs, if the $S = 0$ state is in fact dominating the high y^* values (the low Q values). Instead, we find an almost flat distribution with the first data point abnormally high. The first and last points might be the most affected by possible resonances and final state interactions, so we could choose not to include it in the analysis of the data, but as we can see this would surely yield a different value for R.

The two methods for the study of the FD effect, which we have just described, make use of different measurements and analysis procedures, but both have something in common, their need for MC corrections. The MC simulations play thus a very important role in the study of BE and FD correlations between particles produced in high energy particle collisions, especially in the case of the protons, for which the correlation can only be studied with the help of a reference sample.

One of the most frequently used event generators is the PYTHIA program. This simulator performs the fragmentation or hadronization process according to the Lund string scheme, which depends upon some parameters, described in section 3. These parameters have been tuned by making the results of certain experiments and of the MC simulations come into agreement. The observables usually employed for the tuning are inclusive particle distributions, i.e. distributions of multiplicity, distributions of particle momenta (in the direction of the thrust axis $p_{||}$ and in transverse directions p_t), or distributions in rapidity (defined as $y = \frac{1}{2} \log \frac{E+p_{||}}{E-p_{||}}$, with E being the particle energy); also, event shape data are often used for the fittings. In spite of the number of experimental variables used for the tuning of the MC parameters, the choice for their values is not unique. For example, it is possible to change the values of a and b, the most important parameters in the Lund fragmentation model, in such a way that the MC-simulated inclusive particle spectra remain approximately unchanged, so that we would still find an agreement with the mentioned experimental distributions. However, could such a change in a and b possibly modify the MC simulations of the two-particle correlations?[2]

The main purpose of this thesis is to study the correlations between protons in MC-generated events:

$$C_{MC}(Q) = \frac{MC(Q)}{MC^{mix}(Q)} \tag{10}$$

where $MC(Q)$ represents the MC generated distribution of "real" pairs of protons, belonging to the same events, as a function of $Q = \sqrt{-(p_1 - p_2)^2}$, and $MC^{mix}(Q)$ reads the distribution of pairs of protons coming from differents MC generated events. This correlation is related to the dynamics of the production of the protons in an event. It is expected to show a depletion at low Q due to the fact that two protons cannot be produced as neighbours in rank in the Lund string. In other words, the difference in momenta between the protons of the real pairs cannot be too small, whereas the mixed pairs may have relatively smaller Q values, since their protons come from different and independent events. We will investigate whether this correlation shows noticeable dependence on the parameters a and b, and how a possible dependence $C_{MC}(Q, a, b)$ could affect the values

[2]More exactly, the parameters a and b should be changed together with $k_{\perp c}$, the cut-off value for the gluon transverse momentum that determines the transition from the perturbative to the non-perturbative phase in an e^-e^+ annihilation (see section 3 below), and the average transverse momentum σ of the produced $q\bar{q}$ pairs [18]. This detail will be left for further thorough studies; our time limitations will allow us to study merely the qualitative effect of changing a and b.

obtained for R and λ. It will also be studied if $C_{MC}(Q)$ is influenced by variations in the so-called *popcorn* model (see Sect. 3). Especially interesting are the results found by the DELPHI collaboration in [10], namely that the pp distribution obtained from the MC mixed-events coincides with the MC real pairs distribution, that is to say $C_{MC}(Q) = 1$. We will try to discuss this result after presenting our own simulations.

The thesis is organized as follows. In sections 2 and 3 we provide brief theoretical reviews of the HBT effect and the Lund string fragmentation model. Section 4 contains the MC simulations we performed to study possible influences in the two-proton correlation, and in section 5 we summarize our results.

2 The Hanbury Brown-Twiss effect

The main focus of this section is to review the usual derivation of the HBT effect that leads to equation (1), while explaining the terms *coherence* and *incoherence* introduced previously. The treatment that we give below is in elementary terms; for a thorough theoretical discussion the reader is referred to the article by Gyulassy *et al.* [4].

Let us first consider an experiment in which only one particle is emitted from a distribution of sources localised at different positions, x_j. Each source is characterized by some time-dependent probability amplitude f_j that is a delta function in coordinate space, $f_j\,(\boldsymbol{x}) = f_j\,\delta(\boldsymbol{x} - \boldsymbol{x_j})$. If $\psi_p\,(x)$ is the wave function of the emitted particle, with energy-momentum p, then the probability $P_C\,(p)$ of observing the particle would be:

$$P_C\,(p) = \left| \sum_j \psi_p\,(x_j)\,f_j \right|^2 = \sum_j |\psi_p\,(x_j)|^2 |f_j|^2 + \sum_j \sum_{i \neq j} \psi_p\,(x_j) \psi_p^*\,(x_i) f_j f_i^* \tag{11}$$

We speak of *coherent emission* when there is some distinct phase relation between the wave functions of the sources, so that the sum of cross terms in the equation above do not vanish. All the possible individual emission processes are quantum-mechanically entangled in such a way that it is not possible to determine the initial state by any measurement performed on the final state, as we mentioned in the introduction. Lasers or quantum amplifiers are examples of such coherent sources. On the other hand, the *chaotic* or *incoherent limit* assumes that the phases of the source amplitudes are randomly fluctuating; the average of the phases will tend to be small and can be set to zero if the number of sources is large. Thus the cross terms in eq. (11) vanish and the total probability of detecting the particle becomes $P_I\,(p) = \sum_j |\psi_p\,(x_j)|^2 |f_j|^2$. This is the central assumption pertaining to the HBT effect. Hence, if the nature of the emission is chaotic, each source emits particles independently of the other sources and it is possible to determine exactly in which source an observed particle was produced. This is normally the case for emission from thermal systems.

Suppose now that the wave function of the particle is a plane wave,

$$\psi_p\,(x) \propto \exp\left[\, -i\,(\omega t - \boldsymbol{k} \cdot \boldsymbol{x})\right] = \exp\left[\, -i\,(E \cdot t - \boldsymbol{p} \cdot \boldsymbol{x})\right] = \exp\,(-i\,px) \tag{12}$$

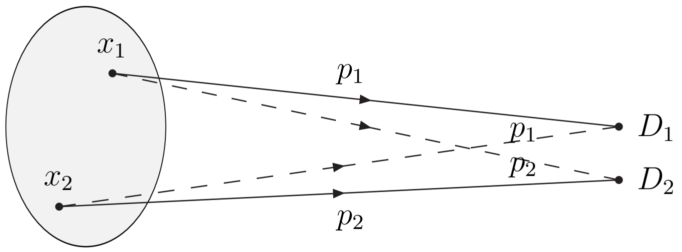

Figure 3: Schematic representation of the two diagrams (one with broken lines, the other with continuous lines) that contribute to the probability amplitude of detecting at points D_1 and D_2 two identical particles produced at points x_1 and x_2 on a source volume.

where we have used natural units, and four-vector notation in the last exponential. Suppose further that the emission points are continously distributed, forming an extensive source volume, so that the sums above will now be replaced by integrals. Then the probability of observing a particle emitted from a coherent source would be

$$P_C\,(p) = \left| \int \psi_p\,(x)\, f_C\,(x)\, dx \right|^2 = \left| \int e^{-i\,p\cdot x}\, f_C\,(x)\, dx \right|^2 = \left| \tilde{f}_C\,(p) \right|^2 \tag{13}$$

where the tilde denotes a Fourier transform. For a chaotic source the probability would be

$$P_I\,(p) = \int |\psi_p\,(x)|^2 |f_C\,(x)|^2\, dx = \int |e^{-i\,p\cdot x}|^2 |f_C\,(x)|^2\, dx = \int \rho(x)\, dx \tag{14}$$

writing $\rho(x) = |f_C\,(x)|^2$ for the source density.

Consider now the simultaneous detection of two identical particles with momenta p_1 and p_2 emitted from two particular points of the source volume, x_1 and x_2. In figure 3 we have represented the two indistinguishable diagrams that interfere in the detection process, which will then be characterized by an amplitude

$$A_{12} = \frac{1}{\sqrt{2}} \left(e^{-i\,p_1\cdot x_1} e^{-i\,p_2\cdot x_2} \pm e^{-i\,p_1\cdot x_2} e^{-i\,p_2\cdot x_1} \right)\; f(x_1) f(x_2) \tag{15}$$

The two-particle wave function must be symmetric (+) or antisymmetric (-) depending on whether we deal with identical bosons or fermions respectively. The probability of observing simultaneously two identical particles produced coherently at any two points of the source can then be written as

$$P_C\,(p_1, p_2) = \frac{1}{2} \left| \int \frac{1}{\sqrt{2}} \left(e^{-i\,p_1\cdot x_1} e^{-i\,p_2\cdot x_2} \pm e^{-i\,p_1\cdot x_2} e^{-i\,p_2\cdot x_1} \right)\; f(x_1) f(x_2)\; dx_1 dx_2 \right|^2 \tag{16}$$

The factor of 1/2 must be included given that the particles are indistinguishable and the sources are related to each other. For bosons (+), we find $P_C{}^b\,(p_1, p_2) = |\tilde{f}_C\,(p_1)\, \tilde{f}_C\,(p_2)|^2$, while the antisymmetrization of the two-fermion wave function leads to a null detection probability, $P_C{}^{f}\,(p_1,p_2) = 0$, meaning that a coherent state cannot be constructed for fermions.

Repeating the above argument for incoherent source emission we find the following coincidence probability

$$
\begin{aligned}
P_I\,(p_1,p_2) &= \int |A_{12}|^2\, dx_1 dx_2 = \int [\,1 \pm \cos[(p_1-p_2)(x_1-x_2)]\,]\; \rho(x_1)\rho(x_2)\; dx_1 dx_2 = \\
&= \left| \int \rho(x)\; dx \right|^2 \pm \int \frac{1}{2} \left[e^{i\,q\cdot(x_1-x_2)} + e^{-i\,q\cdot(x_1-x_2)} \right]\; \rho(x_1)\rho(x_2)\; dx_1 dx_2 = \\
&= \left| \int \rho(x)\; dx \right|^2 \pm \left| \int \rho(x)\; e^{i\,q\cdot x}\; dx \right|^2
\end{aligned}
\tag{17}
$$

with the plus sign for bosons and the minus sign for fermions, as before.

The two-particle correlation $C\,(p_1,p_2) = P(p_1,p_2)/P(p_1)\,P(p_2)$ for bosons and fermions emitted by a coherent or an incoherent source can now be calculated straightforwardly:

$$
\begin{aligned}
&C_C{}^{b}\,(p_1,p_2) = 1 && C_C{}^{f}\,(p_1,p_2) = 0 \\
&C_I{}^{b}\,(p_1,p_2) = 1 + \left| \frac{\int \rho(x)\exp(iqx)\; dx}{\int \rho(x)\; dx} \right|^2 && C_I{}^{f}\,(p_1,p_2) = 1 - \left| \frac{\int \rho(x)\exp(iqx)\; dx}{\int \rho(x)\; dx} \right|^2
\end{aligned}
\tag{18}
$$

Therefore, the correlations associated with the symmetries imposed by quantum mechanics will arise if the emission is totally incoherent, but they will not show up for totally coherent sources. These two limits, however, are not mutually exclusive. The source emission may be constituted by both coherent and incoherent components [14]. Besides, because of limited statistics, the experimental value obtained for the sum of cross terms of eq. (11) usually deviates from zero even for totally incoherent sources. For these reasons, the two-particle correlations may take any values in the ranges $C^{\,b}\,(p_1,p_2) \in (1,2)$ and $C^{\,f}\,(p_1,p_2) \in (0,1)$. In order to accommodate these results, the "chaoticity" parameter λ is normally introduced as a coefficient multiplying the normalized Fourier transform of the source density $\mathcal{R}(q) = \frac{\int \rho(x)\exp(iqx)\; dx}{\int \rho(x)\; dx}$:

$$
C^{b}(p_1,p_2) = 1 + \lambda\,|\mathcal{R}(q)|^2 \qquad\qquad C^{f}(p_1,p_2) = 1 - \lambda\,|\mathcal{R}(q)|^2 \tag{19}
$$

Equations (3) and (4) are readily derived from the formulas above if we assume a spherical symmetric Gaussian distribution for the spatial source density, $\rho(r) = \rho(0)\; e^{-\frac{r^2}{2R^2}}$. Alternative models for the source density may be assumed, but we always find that the correlation is finally parametrised in terms of some parameters describing the dimensions of the source. However, there is an important point to be made. Any model for multiparticle production in high energy collisions predicts a correlation between the position where a particle is produced and the momentum of the particle. It can be proved [15] that if there is a strong correlation between x and p, the sum of cross terms of eq. (11) will explore only a limited range of the source, so that the dimensions obtained from the observed two-particle correlation will not necessarily correspond to the overall size of the source. It is instead the distance apart of production points for which the momentum distributions of the produced particles overlap which will be measured using the BE effect.

The formalism for the derivation of the HBT effect that we have just presented here has severe shortcomings. For example, the assumption has been made that only two particles are produced from the source. Instead of the simple wave function that we have employed to describe the two particles, we would need to use the wavefunction obtained after solving the Schrödinger equation of the many interacting particles produced by the source. This problem, together with the difficulty of including strong and coulomb two-body interactions and of treating higher order correlations, makes this wave function formalism unsuitable for a precise derivation of the particle correlations. Moreover, the coherence emission is not treated adequately and the isospin of the particles is not taken into account. The derivation of the particle correlation could be made within the formalism of quantum field theory [14], which solves these problems and predicts other effects, some of them quite surprising, such as the existence of particle-antiparticle correlations.

3 The Lund Model

Let us first explain briefly the various stages in a high energy particle process, in order to introduce to the unfamiliar reader the context in which the Lund model works. A typical high energy process is representated in Fig. 4.

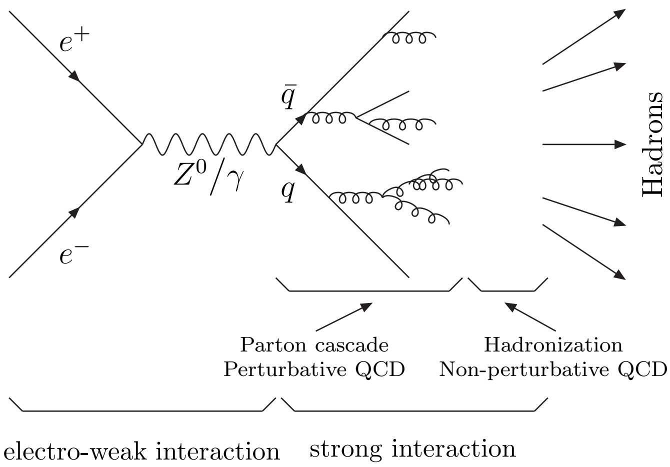

Figure 4: Schematic picture of the various stages in hadronic e^+e^- events.

According to the theory for electro-weak interactions, when an electron and a positron collide they may annihilate into a photon or a Z^0, which in turn may split into a quark q and an antiquark $\bar{q}$. The rest of the process is described by the theory for the strong interaction, called quantum chromo dynamics (QCD). Firstly, the quark and the antiquark radiate gluons, which may radiate additional gluons and split into new $q\bar{q}$ pairs. This parton cascade is described by perturbative QCD-calculations. Such calculations rely on the assumption that quarks and gluons can be considered free particles as long as they move within short distance scales (up to around one fermi). As the parton cascade evolves, the distance scales increase and the momentum transfers between the partons decrease, so that the perturbative QCD approach becomes inapplicable. After this point, a considerable amount of changes seem to occur, since what we observe at the detector level is no longer a shower of independent quarks and gluons but, instead, a large number of hadrons, moving within one or more jets. This hadronization stage should then be explained by some non-perturbative QCD model. One such model that has been very successful when compared with experimental data is the Lund string fragmentation model. The success of the Lund model stems not only from its ability to describe many of the dynamical features of multiparticle production, but also from the fact that the fragmentation of the quarks and gluons is modelled as an iterative stochastic process that readily lends itself to a computer Monte Carlo implementation like PYTHIA.

3.1 Basic Concepts

The strong force field or *colour field* between two partons is believed to be stretched in the form of a small one-dimensional tube. This idea is based on the observation that the force-mediating gluons themselves interact with each other. Since they are massless, it is energetically favorable for a spatial region to be filled with a bound gluonic state rather than being empty. The vacuum becomes then a "soup" of bound gluons, where the colour field lines between two quarks would require an infinite energy to "push away" the gluons and spread out over all space.

The tube-like colour field spanned between a quark and an antiquark moving in opposite directions is approximated, in the Lund model, by a massless relativistic string (MRS) with a constant amount of energy per unit length $\kappa \simeq 1\,GeV/fm$. For simplicity, the endpoint quarks are assumed to be massless (and thus to be moving at the speed of light, so that $x = \pm\, t$ and $E = \pm\, p$, for the position x, energy E and momentum p of each particle), although the dynamics we are going to consider is basically independent of this assumption [16]. It should also be remarked that the Lund model makes use of semi-classical arguments, which esentially describe very precisely the dynamics of the system in the longitudinal degree of freedom (direction of the colour force, x axis) if the energies involved are large. (This is easily understandable from the fact that the Heisenberg uncertainty principle $\Delta x \cdot \Delta p_{||} \geq 1$, in the rapidity variable $y = \frac{1}{2} \log \frac{E+p_{||}}{E-p_{||}}$ (which satisties $\Delta y = \Delta p_{||}/E$), takes the form $\Delta x \cdot \Delta y \geq 1/E$.)

It is clear from the hamiltonian of the $q\bar{q}$ system $H = T + V = |p_1| + |p_2| + \kappa |x_1 - x_2|$ that, as the quarks separate from each other, their initial energies are gradually transferred to the colour field confined between them. If the original energy of the pair is not too large, the quarks presently run out of energy and are dragged back by the field. Eventually the quarks meet again, but with exchanged modes of motion as compared to the starting point. This yoyo mode of the MRS is the simple pictorical approach that the Lund model provides for stable hadrons.

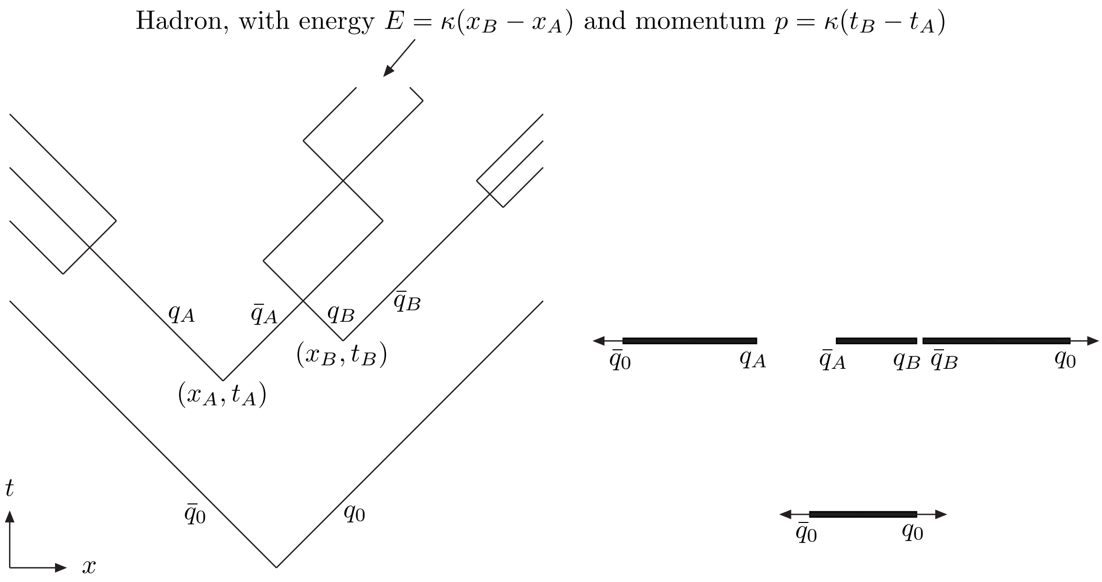

Figure 5: String fragmentation that occurs when q_0 and $\bar{q}_0$ move with large energies in opposite directions. The thick lines at the right side of the picture indicate where the colour field is non-vanishing.

Let us now suppose that the original $q_0\bar{q}_0$ state is produced with a large amount of energy. The quarks from the pair still cannot be released, since the potential between the quarks is linearly rising and thus, an infinite amount of work would be needed to separate them. (In this way the Lund model nicely accounts for the fact that no free quarks have been experimentally observed so far.) What actually occurs for large initial kinetic energies, according to this model, is that the energy stored by the colour field between the quarks gets so large that it becomes energetically possible for the string to break up by the creation of a new pair $q_A\bar{q}_A$, which will together contain the internal quantum numbers of the vacuum. The new quarks q_A and $\bar{q}_A$ immediately start to separate (moving towards $\bar{q}_0$ and q_0 respectively) owing to the forces exerted by the two adjoining string pieces, while the total string field between them vanishes, as shown in Fig. 5. Provided that the two independent string pieces have enough energy, they will in turn decay into smaller pieces, which will iteratively continue the fragmentation process until only ordinary hadrons remain.

3.2 The unique breakup distribution. Parameters a and b

We will now review the main ideas used to derive the unique fragmentation function in the Lund model. Consider the meson state of Fig. 5 formed from the quarks q_B and $\bar{q}_A$. Its mass will be given by $m^2 = E^2 - p^2 = \kappa^2(x_B - x_A)^2 - \kappa^2(t_B - t_A)^2$, and thus it will be real only if the distance between the production points (also called vertices) A and B is spacelike. In this way, a Lorentz boost can be performed to another frame in which the vertex B will seem to appear earlier than vertex A. Since the same causal disconnection is found

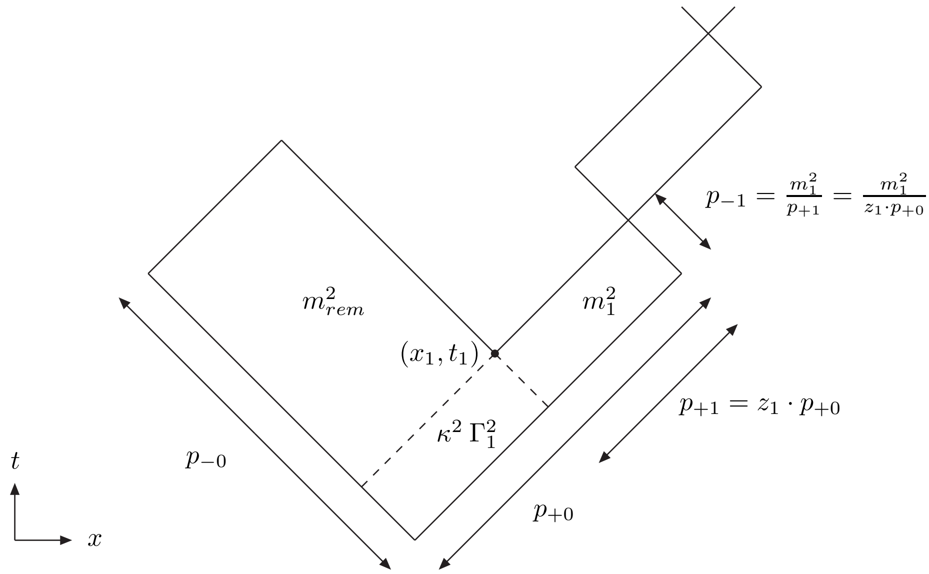

Figure 6: Production of the first-rank particle, with mass m_1, from the original quark q_0 and the antiquark created at vertex (x_1, t_1). After this production, the square mass of the remaining system m^2_{rem} is given by the area indicated in the diagram.

between all adjacent vertices, we can draw the conclusion that no vertex is more significant than any other, in other words, that all the vertices are of the same dynamical status. A convenient ordering of the produced particles must then be *rank-ordering*, instead of, for example, ordering in the time-coordinate of productions. The first-rank meson is normally defined as the one containing the original quark q_0 and the antiquark produced at the first vertex along the lightcone (the vertex closest to the endpoint q_0), while the quark from this vertex plus the antiquark from its adjacent vertex would form the second-rank meson, etc.

Let us consider a reference system for which the first-rank meson is the first particle to be produced, and try to calculate the mass of the remaining system after its production. It is convenient for this purpose to introduce the lightcone variables in momentum space $p_\pm = E \pm p$, and the Lorentz-invariant set of variables $z_{\pm j} = p_{\pm j}/W_{\pm j} \in (0,1)$. The variables p_{+j} and p_{-j} are the lightcone components carried by the antiquark and the quark, respectively, at the time of their first meeting to form the rank-j yoyo-hadron, while W_{+j} and W_{-j} are the total available lightcone energy-momenta of the system at the moment of the production of the rank-j particle. The positive and negative lightcone components are obviously linked by the mass-shell condition $p_{+j}p_{-j} = m_j^2$, m_j being the mass of the rank-j particle. Therefore, the positive energy-momentum component taken by the first-rank hadron is $p_{+1} = z_{+1}\, p_{+0} \equiv z_1\, p_{+0}$ (where p_{+0} is the positive lightcone of the original quark q_0), the negative component is $p_{-1} = \frac{m_1^2}{p_{+1}} = \frac{m_1^2}{z_1 \cdot p_{+0}}$, and thus, the remaining mass of the system will be given by:

$$\begin{aligned} m^2_{rem} &= (p_{+0} - p_{+1})\,(p_{-0} - p_{-1}) = (1 - z_1)\, p_{+0}\,(p_{-0} - p_{-1}) = \\ &= (1 - z_1)\, p_{+0}\, p_{-0} \; - \; (1 - z_1)\, p_{+0}\, p_{-1} \end{aligned} \tag{20}$$

The last term in this equation clearly corresponds to the area of the region below the first vertex, as shown in Fig 6, which is proportional to the squared proper time of the vertex

$\Gamma_1^2 = t_1^2 - x_1^2$; more precisely, we have the relation $(1 - z_1)\, p_{+0}\, p_{-1} = \kappa^2\, \Gamma_1^2$. Provided that this proper time is a finite quantity much smaller than the original mass $m_0 = \sqrt{p_{+0}\, p_{-0}}$, then equation (20) becomes $m_{rem}^2 \approx (1 - z_1)\, p_{+0}\, p_{-0}$. The remainder system can then be considered similar to the original system apart from a scaling down of the positive lightcone component, by a factor $1 - z_1$, and the quark q_1 at the endpoint instead of the original q_0. The same considerations apply for the last-rank meson, except that the scaling is performed on the negative lightcone component, by a factor $1 - z_{-1} = 1 - p_{-1}/p_{-0}$.

The iterative fragmentation scheme of the Lund model stems from two basic assumptions. The first one is related to the example above; it reads that even when the energy of the original pair becomes very large the proper times of the vertices stay finite, so that in the centre of phase space (far from the endpoints q_0 and $\bar{q}_0$) there is always much energy left in the string for the production of hadrons. If the initial energy is large, the string will decay into many yoyo-hadrons, so that the ones produced in the centre will be essentially independent of the many steps z_j (partitions of energy-momentum) that occur before their own production. The string decay process corresponds then to a stochastic process, where each vertex in the process is determined solely by the previous starting point and by the probability of taking a particular step along the lightcone. The second main assumption is that the final-state hadron production process should be statistically the same if we describe it in terms of steps along the positive or along the negative lightcones (left-right symmetry). Let us denote by $f(z) \cdot dz$ the probability that a hadron with mass m takes a fraction between z and $z + dz$ of the energy-momentum remaining in the system at the moment of its production. With the assumptions above, the distribution $f(z)$ can be shown to have the following functional form

$$f(z) = N \frac{1}{z} (1 - z)^a \exp(-\frac{b \cdot m^2}{z}) \tag{21}$$

while the distribution $H(\Gamma)$ for the proper times of the production vertices will be given by

$$H(\Gamma) = C\, \Gamma^a \exp(-b\Gamma) \tag{22}$$

where the quantities N and C are normalisation constants, and a and b are the free parameters we mentioned in the introduction. The parameter b must be the same for all vertices, whereas a may in principle have different values in different vertices, depending upon the flavour quantum numbers of the pair produced in them. Experiments suggest that a can nevertheless be assumed to have the same value everywhere, in the intervals $0 \le a \le 2$ [17].

It is easy to convince oneself that an increase in the values of a and b will modify the separation in rapidity between neighbouring hadrons in the string. The separation between hadron j, produced from the available energy-momentum W_+, and hadron $j+1$ is given by

$$\delta y = y_j - y_{j+1} = \frac{1}{2} \log \frac{p_{+j}}{p_{-j}} - \frac{1}{2} \log \frac{p_{+\,j+1}}{p_{-\,j+1}} = \frac{1}{2} \log \frac{(p_{+j})^2}{m_j^2} - \frac{1}{2} \log \frac{(p_{+\,j+1})^2}{m_{j+1}^2} =$$

$$= \log \frac{z_j W_+}{m_j} - \log \frac{z_{j+1}(1 - z_j) W_+}{m_{j+1}}$$

Assuming that both hadrons have the same mass $m_j = m_{j+1} = m$, we find

$$\delta y = \log \frac{z_j}{z_{j+1}(1-z_j)} \tag{23}$$

From this expression we can readily find the distribution of such rapidity separations

$$P(\delta y) = \int_0^1 dz \int_0^1 dz'\, f(z)\, f(z')\, \delta \left(\delta y - \log \frac{z}{z'(1-z)} \right) \tag{24}$$

This distribution can only be solved by numerical methods, but we can predict, without performing the actual calculation, that $P(\delta y)$ becomes narrower for larger values of a and b, since this is the behaviour of the fragmentation function $f(z)$ inside the integrals. In this way, the ordering in rapidity becomes more like the one in rank, meaning that, if we increase a and b while keeping the average rapidity separation $<\delta y>$ unchanged, the distribution of energy-momentum differences Q between the produced hadrons will exhibit a deeper depletion at low Q values.

3.3 Baryon production. The *popcorn* mechanism

With the brief introduction of the Lund model that we have provided above, we have only been able to describe the production of mesons, although we know that a non-negligible amount of baryons and antibaryons is also created in e^+e^- annihilations. Basically there are two models to explain the production of baryons within the Lund fragmentation picture. The simplest production mechanism, known as the *diquark model*, relies on the assumption that a diquark-antidiquark pair in a $\bar{3}$-3 colour state may tunnel out from the vacuum like a heavy quark pair. If a qq-$\overline{qq}$ pair is produced in a vertex of the string, then they will combine with the quark and the antiquark produced at the adjacent vertices, giving rise to a baryon and an antibaryon, colour-neutral and neighbours in rank. Within this model, the average rapidity separation between baryons and antibaryons is expected to have a small value around $|y_b - y_{\bar{b}}| \simeq 0.5$, which is unfortunately far away from the experimental result $|y_b - y_{\bar{b}}| \simeq 1.3$. Beside this problem, diquarks are not considered basic quanta of the QCD colour field, and it is not easy to explain how such non-fundamental quanta may tunnel out from the vacuum. These drawbacks are solved in the so-called *popcorn model*.

We stated before that a $q\bar{q}$ pair produced at some vertex in the string breaks the colour field between them. The assumption was then made that the new pair contains the same colour as the original $q_0\bar{q}_0$. In the popcorn scenario the production of a $q\bar{q}$ pair with a different colour is also allowed. Imagine for example that a $b\bar{b}$ pair is created inside an original $r\bar{r}$ field. At one end we would find a combination of quarks b and r, behaving like a $\bar{g}$ state, whereas at the other end we would have the antiquarks $\bar{b}$ and $\bar{r}$ with combined colour g. Therefore, the colour field spanned between the new wrong-colour pair would be a $g\bar{g}$ field, with the same strength but oppositely directed as compared to the $r\bar{r}$ field outside the $b\bar{b}$ pair. The wrongly-coloured quarks, also called curtain quarks, are thus pulled with the same magnitude of force in the two directions and energy is neither gained nor lost as they slide back and forth in the string. Curtain quarks can live for a short period, given by the Heisenberg uncertainty principle, normally causing only a temporary colour fluctuation in the string. However it may occur that another $q\bar{q}$ pair with the appropriate colour, a $g\bar{g}$ pair in the example above, breaks the field between the curtain quarks, producing an effective diquark-antidiquark pair, which will yield a baryon-antibaryon pair, as in the diquark model. This process is represented in the right-hand side of Fig. 7. We must realize that in the popcorn model diquarks are produced in a stepwise manner and there is no need for requiring that two quarks and two antiquarks tunnel out together from the vacuum. Furthermore, the baryon and the antibaryon do not need to be produced as neighbours in rank, since the colour fluctuation region may also break up in more than one $q\bar{q}$ pair, producing one or more mesons between the baryon and the antibaryon, as shown in the picture below. In this way the baryon-antibaryon rapidity separation becomes greater on average than in the diquark model. The experimental data thus tend to support the popcorn scenario.

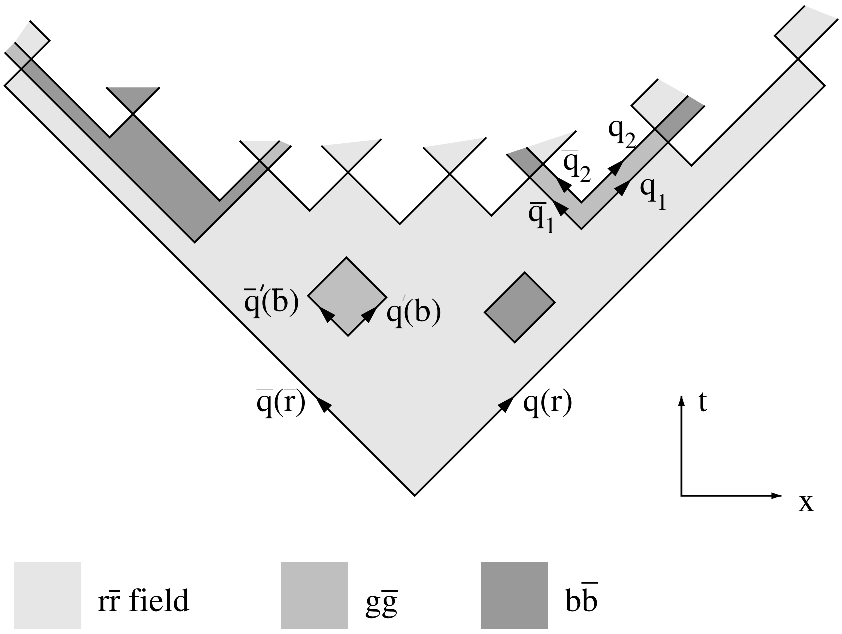

Figure 7: Representation of colour fluctuations in the string. The wrongly-coloured pair $q_1(b)\bar{q}_1(\bar{b})$ together with $q_2(g)\bar{q}_2(\bar{g})$ form an effective diquark-antidiquark pair, yielding a baryon and an antibaryon, neighbours in rank. At the left-hand side we show the production of a baryon and an antibaryon with a meson between them, arising from two breakups in a colour fluctuation region.

4 MC simulation of proton correlation

4.1 Algorithm and results

We will now explain the program we made to get the MC proton correlation, $C_{MC}(Q) = MC(Q)/MC^{mix}(Q)$. First, we call a routine of PYTHIA 6.2 [12] to generate complete events $e^+e^- \to hadrons$. We generate 5 million events at a total energy of 91 GeV, and for each particle produced we record the type of particle, energy-momentum, mass, origin (whether it comes directly from the Lund string or from any decay) and possible resonance. For each event we look for the protons produced, we pair them in all possible combinations without repetitions (i.e. we would get $1+2+\ldots+(n-1)$ pairs in an event with n protons), and we calculate the Q values of the couples, which we use to construct a histogram. After looping over all the events, the final histogram of Q is normalized, becoming $MC(Q)$.

In order to find the Q distribution of mixed pairs $MC^{mix}(Q)$, we start by doing a thrust analysis of every event. The parameter thrust T is defined by

$$T = \max_{|\boldsymbol{n}|=1} \frac{\sum_i |\boldsymbol{n} \cdot \boldsymbol{p_i}|}{\sum_i |\boldsymbol{p_i}|} \tag{25}$$

where $\boldsymbol{p_i}$ is the spatial momentum of the particle i and $\boldsymbol{n}$ is the unit-vector for which the maximum is attained. The quantity T ranges from $T = 1/2$ for an isotropic event to $T = 1$ for a 2-jet event. The $\boldsymbol{n}$ vector defines the direction of the *thrust axis*. The so-called *major axis* is calculated with eq (25) similarly, replacing $\boldsymbol{n}$ by $\boldsymbol{n}_{major}$, perpendicular to $\boldsymbol{n}$. After the thrust analysis, we perform a rotation of the event to sit the thrust axis along the z direction and the major axis along the x direction. All the events are thus oriented similarly. Our mixing procedure consists of pairing the protons in an event with the protons in the previous event. (Each event is independent of preceding ones, so this procedure mixes protons randomly). We are again careful not to count the pairs twice, so that the number of pairs we would get from an event with n_j protons and an event with n_{j-1} protons would just be $n_j \times n_{j-1}$. In this way the (spatial) momentum spectrum of the protons belonging to the real pairs is identical by construction to the momentum spectrum of the protons in the mixed events.[3] The distribution $MC^{mix}(Q)$ is analogously found after normalizing the histogram obtained with the Q values of all mixed pairs.

The Q histograms of real and mixed pairs of $\bar{p}\bar{p}$ and $p\bar{p}$ have also been simulated for comparison.

[3] Very often in the analysis of experimental data, the event mixing is constructed by pairing each proton of a real pair with the protons of the real pairs in all other events. This is known as "blind-mixing" and it could affect the level of agreement between the MC single particle momenta distribution and the data distribution. As an example, consider two events with three and two protons respectively. The protons in the real pairs of the first event, $(12, 13, 23)$, and of the second event, $(\tilde{1}\tilde{2})$, would combine to give 12 mixed pairs (instead of the 6 pairs we get with our mixing): $(1\tilde{1}, 1\tilde{2}, 2\tilde{1}, 2\tilde{2}, 1\tilde{1}, 1\tilde{2}, 3\tilde{1}, 3\tilde{2}, 2\tilde{1}, 2\tilde{2}, 3\tilde{1}, 3\tilde{2})$. Thus, while the protons 1,2 and 3 are weighted by a factor of four, the protons $\tilde{1}$ and $\tilde{2}$ are given more importance, they are weighted by a factor of 6. This problem has been commonly corrected by reweighting the simulated protons with the ratio of numbers of protons in data and in simulation for a given momentum bin. See reference [9] for an example.

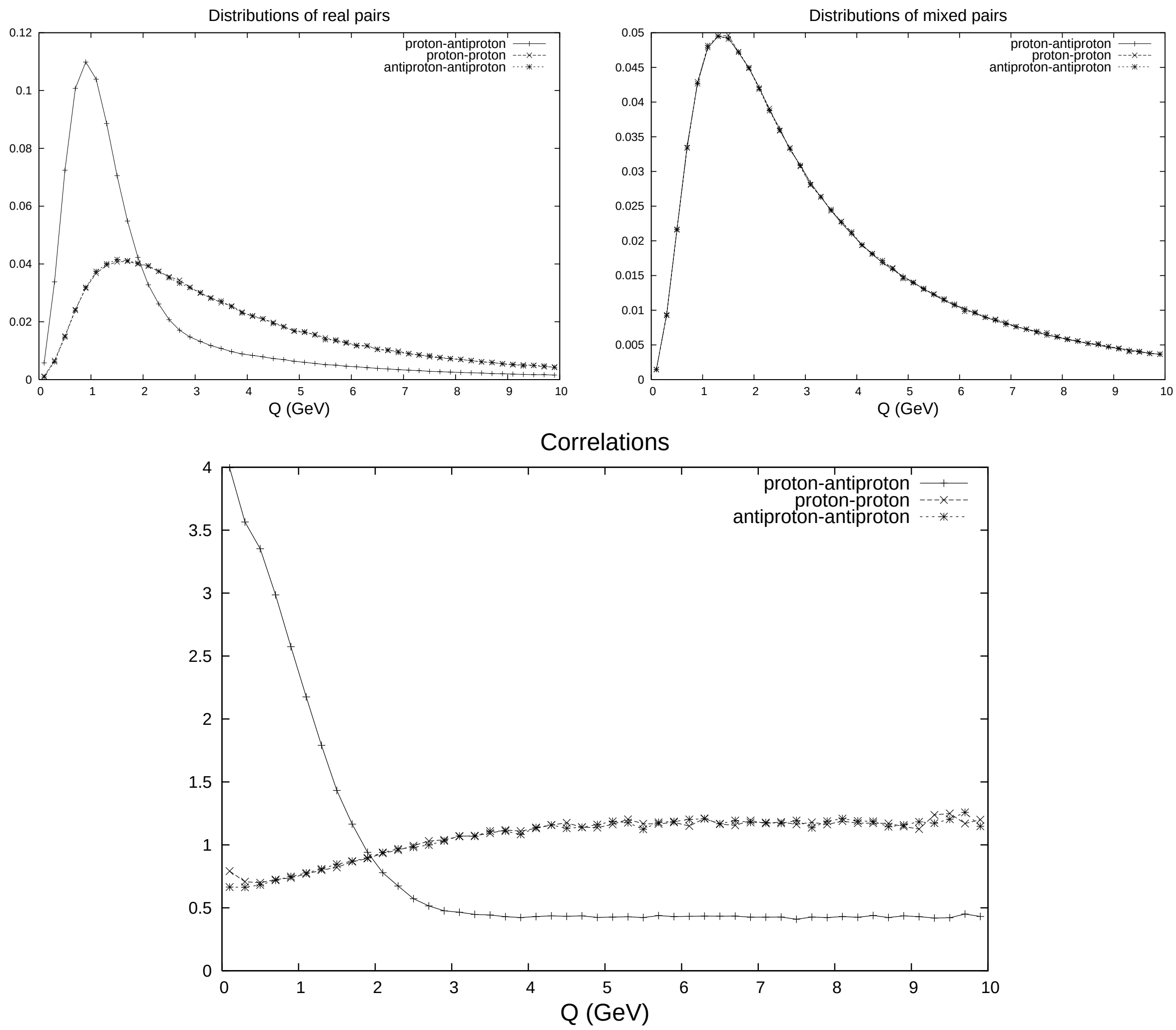

Figure 8: Normalized Q histograms for "real" and "mixed" pairs $p\bar{p}$, pp and $\bar{p}\bar{p}$, and MC correlations $C_{MC}(Q)$ between the constituents of the pairs.

In our simulations, the parameters for the fragmentation and decay treatment are left with their default values [12], except for the variable which describes the baryon production. Here we assume a popcorn scenario with an extra suppression of diquark vertices, which is an improved version of the popcorn model.

In Fig 8 we have plotted the distributions $MC(Q)$, $MC^{mix}(Q)$ and the correlation $C_{MC}(Q)$ for $p\bar{p}$, pp and $\bar{p}\bar{p}$ pairs. The production of $p\bar{p}$ pairs in an event shows an enhancement at low Q values relative to the production of like-sign pairs. This is understandable according to the Lund fragmentation picture, since a proton and an antiproton can be produced as neighbours in rank, while two protons (antiprotons) must have at least one antibaryon (baryon) produced in between. The mixed-event distributions are identical regardless of the pairs involved, which simply means that the single particle spectrum is

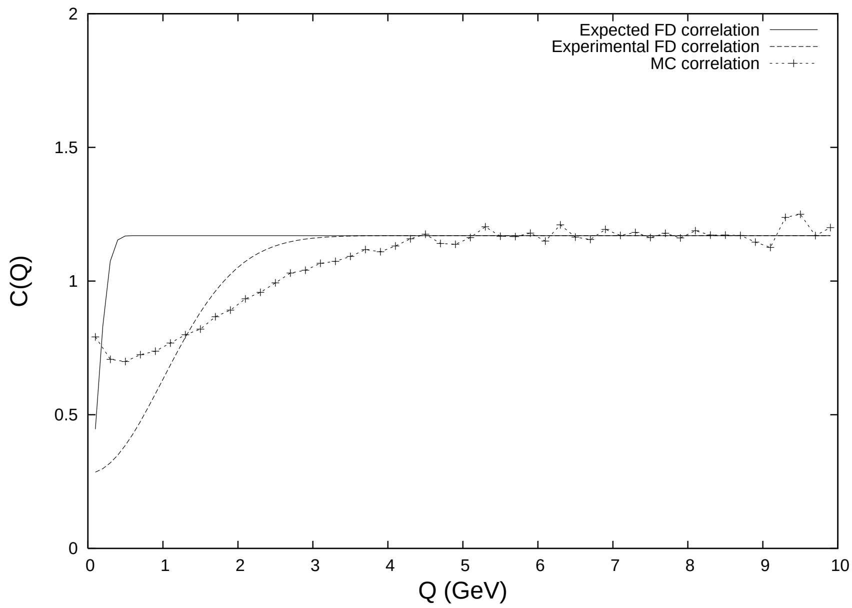

Figure 9: Two-proton MC correlation, $C_{MC}(Q) = \frac{MC(Q)}{MC^{mix}(Q)}$, as compared to the FD correlation function $C(Q) = \mathcal{N}[1 - \lambda \exp(-R^2Q^2)]$, with $\lambda = 0.76$ and $R = 0.14\ fm$ representing a typical experimental curve, and the values $\lambda = 0.76$ and $R = 1\ fm$ for the typical correlation we would expect if the proton "source radius" in e^+e^- annihilations was equal to the meson "source radius" measured in earlier experiments.

identical for protons and antiprotons. The resulting correlations for pairs of protons and pairs of antiprotons are alike (the small difference at the first bins is due to statistical uncertainties and vanishes when increasing the number of events) and they resemble the shape of the FD correlation $C(Q)$ except for the depletion being broader, as represented in Fig. 9.

4.2 Modelling Fermi-Dirac correlations

The Lund model, as any other non-perturbative QCD model for multiparticle production, does not account for quantum mechanical effects, since it only considers probabilities, and not amplitudes, for the production processes. In spite of this, the BE phenomenon can be modelled with several different algorithms that reweight or perturb the MC simulated events so that the two-particle correlation acquires the shape of eq. (3). We will now very briefly describe one successful way of simulating BE correlations by a local reweighting strategy, presented in [19]. The main idea is to generate a MC event normally (with unit weight) and obtain a Q distribution of identical-boson pairs, and then to shift slightly the Q value of each pair to $Q + \delta Q$ so that the original Q distribution is enhanced by a factor $f(Q)$ of the form of eq. (3). If the original Q distribution is assumed to be given by phase space $d^3p/E \propto Q^2dQ/\sqrt{Q^2 + 4m^2}$, then an appropriate shift $\delta Q < 0$ for a given pair can be found as the solution to the following equation

$$\int_0^Q \frac{q^2 dq}{\sqrt{q^2+4m^2}} = \int_0^{Q+\delta Q} f(Q) \frac{q^2 dq}{\sqrt{q^2+4m^2}} \tag{26}$$

This shift δQ is calculated for all pairs, and it is usually translated into shifts of the three-momenta of the pair-constituents. Since a given particle will normally belong to several pairs, the total shift of its momentum will be given by the composant of several different shifts. This procedure ensures momentum conservation, but not energy conservation. In order to preserve the total energy, a rescaling of all three-momenta is performed, multiplying them by a common factor close to unity. The distribution of Q obtained after shifting and rescaling the three-momenta of all identical bosons will now include the BE effect, and it will be different and, further, independent from the function $f(Q)$ we choose as an input.

It would be convenient to have also a good method for simulating FD correlations. As an attempt, we have modified the algorithm mentioned above so as to include a function $f(Q)$ of the form of eq. (4), correponding to a positive δQ shift. The resulting modelled FD correlation has been plotted in Fig. 10 for two different input functions $f(Q)$. Since there are very few protons produced in an event, the modelled correlation differs only slightly from $f(Q)$. Hence, a typical proton source radius cannot be predicted from this algorithm.

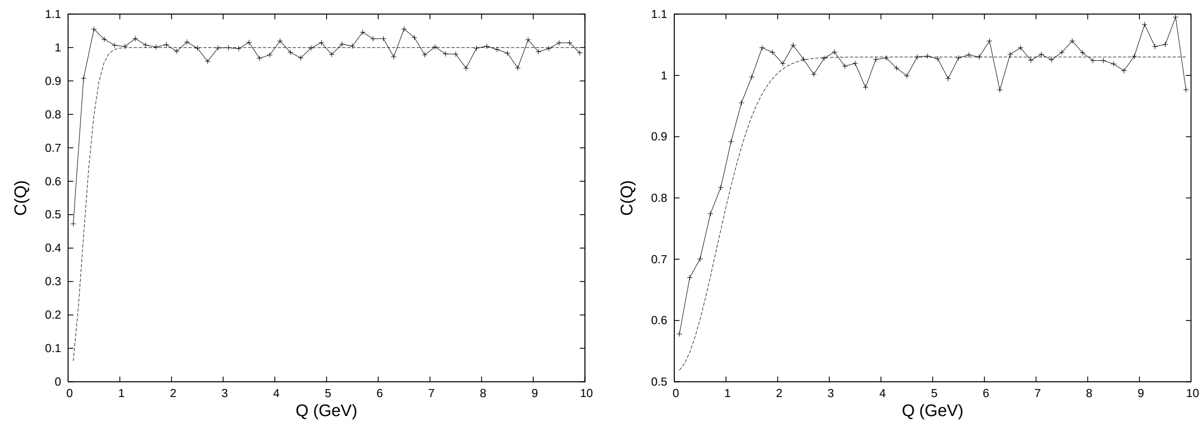

Figure 10: Modelled FD correlations (with crosses) compared to the input function $f(Q) = \mathcal{N}[1 - \lambda \exp(-R^2Q^2)]$ with the values $R = 1\, fm$, $\lambda = 1$ (left) and $R = 0.17\, fm$, $\lambda = 0.5$ (right).

4.3 Influence of the parameters a and b of the Lund fragmentation model

The Lund model states that the distribution of rapidity separations between neighbouring hadrons (24) becomes narrower for larger values of a and b. This means that, if we increase a and b so that the total multiplicity remains the same, the particle distributions from the sources will have smaller overlapping regions and, consequently, the MC correlations will show an extra depletion at low Q.

In this subsection we will study the importance of this effect by simulating the proton correlation for different values of a and b. These values should be changed carefully so that the average event multiplicity remains roughly constant.[4] The average multiplicity could be calculated by dividing the rapidity width of the whole string (proportional to the logarithm of the total energy) by the average width of the rapidity distribution $<\delta y>$. However, from eq. (24) we cannot find a simple analytical result for $<\delta y>$, and thus we do not have a handy expression which relates the average multiplicity of an event with the parameters a and b. As an approximate alternative we will try to keep constant the average vertex proper time, which is closely related to the multiplicity. The average vertex proper time is given by

$$<\Gamma>= \frac{\int_0^\infty \Gamma^a \exp(-b\Gamma)\Gamma d\Gamma}{\int_0^\infty \Gamma^a \exp(-b\Gamma) d\Gamma} \tag{27}$$

Assuming that a is an integer we find:

$$<\Gamma>= \frac{\left(-\frac{\partial}{\partial b}\right)^{a+1}\int_0^\infty \exp(-b\Gamma)d\Gamma}{\left(-\frac{\partial}{\partial b}\right)^{a}\int_0^\infty \exp(-b\Gamma)d\Gamma} = \frac{\left(-\frac{\partial}{\partial b}\right)^{a+1}\frac{1}{b}}{\left(-\frac{\partial}{\partial b}\right)^{a}\frac{1}{b}} = \frac{\frac{(a+1)!}{b^{a+2}}}{\frac{a!}{b^{a+1}}} = \frac{a+1}{b} \tag{28}$$

We will only compare here events with similar mixed distributions. In Fig. 11 we present the mixed pp distributions for the pairs of a and b values we have chosen, corresponding to $<\Gamma>\approx 2.2\, GeV^2$. This is the average vertex proper time obtained with the default values $a = 0.3$ and $b = 0.58\, GeV^{-2}$. There are a few (a, b) values which satisfy $<\Gamma>\approx 2.2\, GeV^2$ but have been excluded due to the clear deviation of their corresponding MC mixed distributions from that obtained with the default $a = 0.3$ and $b = 0.58\, GeV^{-2}$. Examples of these omitted pairs are $a = 1.24$ and $b = 1\, GeV^{-2}$ or $a = 2$ and $b = 1.34\, GeV^{-2}$; the latter has been plotted in Fig. 11 as an illustration.

The pp MC correlations found for these values of a and b are shown in Fig. 12. The depletion is clearly affected, becoming deeper and narrower for larger values of a and b.

Now, it would be interesting to study the influence of a and b on the proton FD correlations found by the ALEPH, OPAL or DELPHI collaborations. It is not possible for us to make an accurate calculation, since we do not know all the details concerning the experimental setups and processes for particle identification, which were included in their MC simulations used for the data analysis; instead we will just do a rough estimation. Using

[4]More exactly, a and b should be changed together with two other parameter of the Lund model so that all inclusive event distributions remain the same, as we pointed out in the introduction.

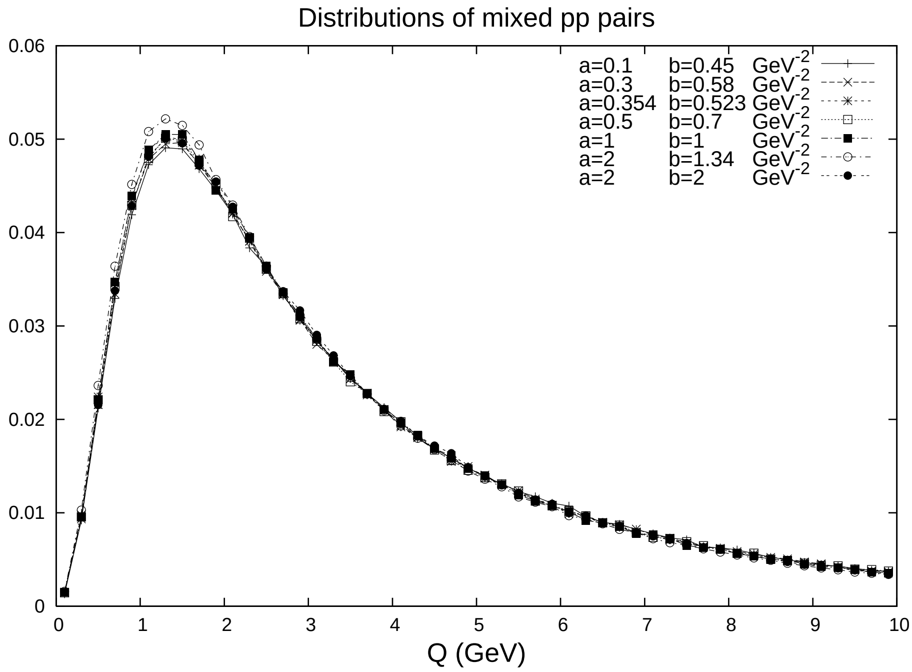

Figure 11: Normalized Q histograms of "mixed" pp pairs for different a and b values.

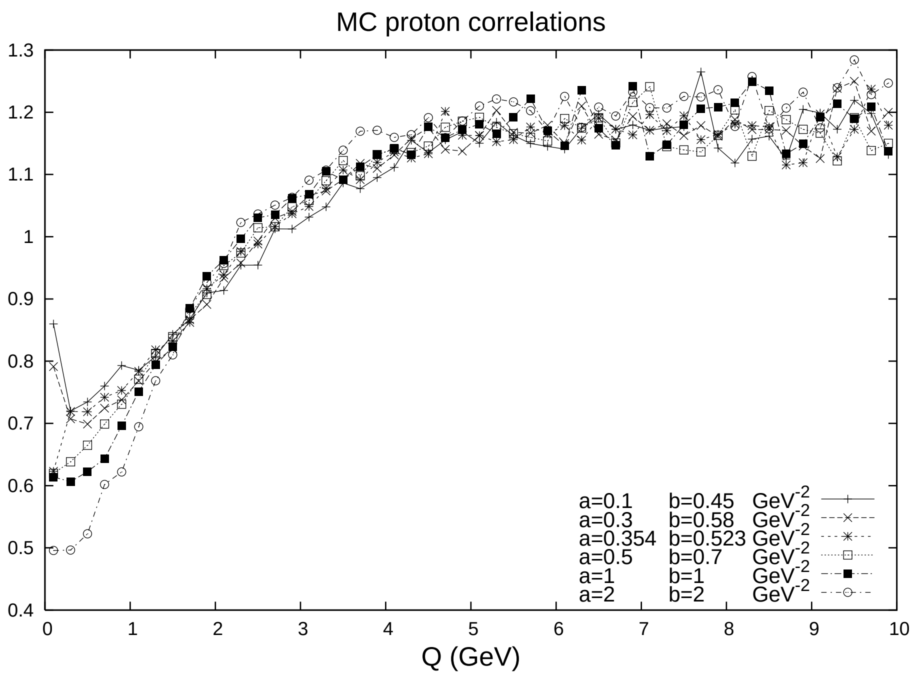

Figure 12: MC correlations $C_{MC}(Q)$ of pp pairs for different a and b values.

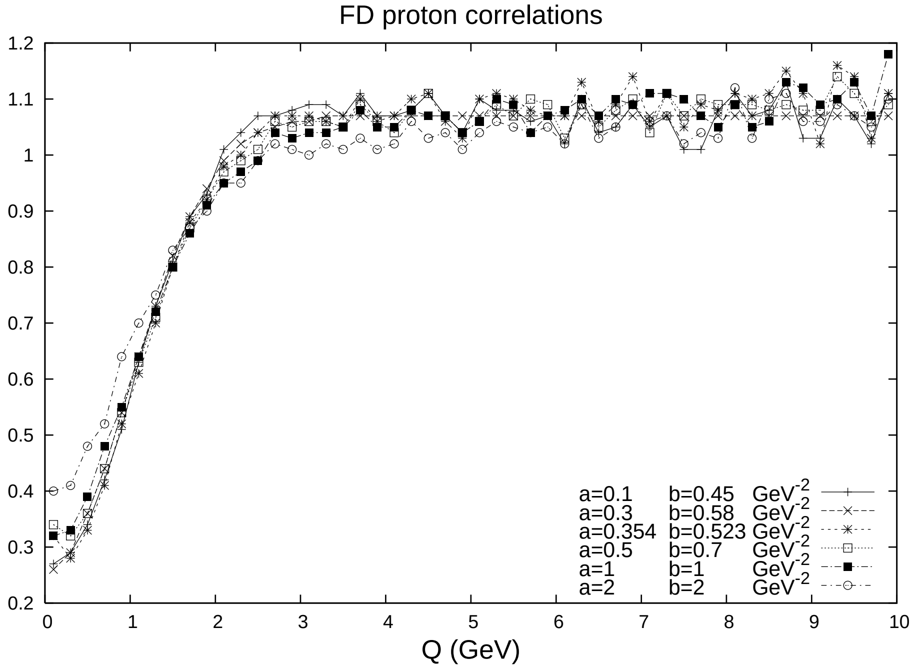

Figure 13: Estimation of the proton FD correlation for different a and b values.

the values R and λ obtained by the OPAL collaboration, for example, and equation (4), we construct a FD correlation which will be referred to as $C^{old}(Q)$

$$C^{old}(Q) = 1 - 0.76 \cdot \exp\left[-Q^2\left(\frac{0.142 \cdot 2\pi}{1.239842}\right)^2\right] \tag{29}$$

We assume that the MC simulation they used for the analysis is the one we performed with the default values $a = 0.3$ and $b = 0.58 GeV^{-2}$, which was shown in the last subsection. The results of this simulation will be called $MC(Q)^{old}$, $MC^{mix,\,old}(Q)$ and $C^{old}_{MC}(Q)$ hereafter. Hence our assumption reads

$$C^{old}(Q) = \frac{N(Q)}{MC(Q)^{old}} \tag{30}$$

N(Q) being the hypothetical measured Q distribution of real pp pairs. Using expression (29), the FD correlations corresponding to other a and b values can then be easily found as follows

$$C^{new}(Q) = C^{old}(Q) \cdot \frac{MC(Q)^{old}}{MC(Q)^{new}} \tag{31}$$

The resulting FD correlations are shown in Fig. 13. Obviously an increase in the a and b values gives rise to opposite effects in the FD correlations and in the MC correlations, but the former are patently less influenced by these changes in a and b.

The plotted FD correlations have been fitted to eq. (4) in order to estimate the range of uncertainty of the parameters R and λ. The values obtained from the fittings are presented

a	$b\ (GeV^{-2})$	$R\ (fm)$	λ
0.1	0.45	0.142 ± 0.003	0.772 ± 0.015
0.3	0.58	0.142	0.76
0.354	0.523	0.132 ± 0.003	0.754 ± 0.015
0.5	0.7	0.131 ± 0.003	0.719 ± 0.011
1	1	0.127 ± 0.003	0.699 ± 0.014
2	2	0.130 ± 0.004	0.609 ± 0.015

Table 2: Values of R and λ obtained from equations (31) and (4) for different a and b values.

in table 2. R and λ values have also been estimated assuming that $C^{old}(Q)$ is the double ratio

$$C^{old}(Q) = \frac{N(Q)}{N(Q)^{mix}} \Bigg/ \frac{MC(Q)^{old}}{MC(Q)^{mix,\,old}} = \frac{N(Q)}{N(Q)^{mix} \cdot C^{old}_{MC}(Q)} \tag{32}$$

so that the FD correlations are obtained with the following formula

$$C^{new}(Q) = C^{old}(Q) \cdot \frac{C^{old}_{MC}(Q)}{C^{new}_{MC}(Q)} \tag{33}$$

The results found in this way agree, within errors, with those shown in table 2.

In conclusion, increasing the values of a and b in such a way that the ratio $(1+a)/b$ and the distribution of mixed pairs remain roughly invariant, apparently decreases the value of R by only a small percentage; in our case $\Delta R/R = 10.5\%$ ranging from $a = 0.1$ to $a = 1$. With eq. (33) we have also estimated R and λ for some other values of a and b

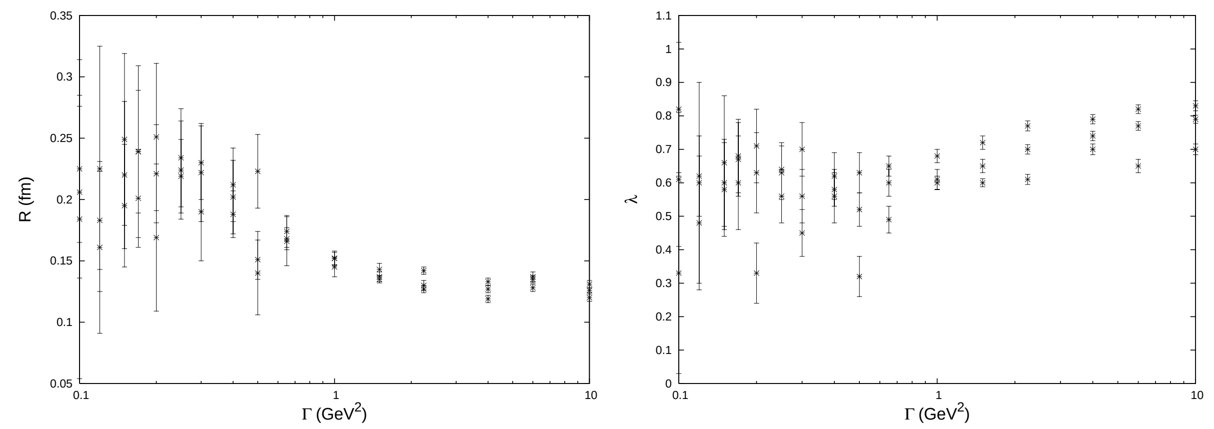

Figure 14: Values of R and λ obtained from eq. (33) and (4) for different ratios $(1 + a)/b$. For each chosen value of $(1 + a)/b$, three calculations have been performed, corresponding to $a = 0.1$, $a = 1$ and $a = 2$. The y-error bars at each data-point indicate the uncertainties in the fittings to eq. (4).

corresponding to different average proper times <Γ> and different mixed distributions. We found that higher multiplicities seem to be related to lower R values, as shown in Fig. 14. The highest R value we obtained was $R = (0.25 \pm 0.06)\, fm$, for $a = 0.1$ and $b = 7.33 GeV^{-2}$ and also for $a = 2$ and $b = 15\, GeV^{-2}$. This value is still too low as compared to the proton radius. In the following section we will study some other possible sources of error in the MC simulations.

4.4 Other possible influences on the MC correlations

The success of a particular baryon-production model is usually measured in terms of the rapidity difference and the transverse momentum correlation between a baryon B and an antibaryon $\bar{B}$ that are neighbours, or close to neighbours in rank. However, the depletion at low Q values due to the FD effect also affects these quantities, and since we do not know for certain the strength of the FD effect, we have some uncertainty in the election of the most suitable model for baryon production. In table 3 we present the values of R and λ obtained from the double ratio of eq. (33) and a fit to eq. (4) for different baryon-production scenarios. The decrease of the FD correlation strength in the order *diquark model – Popcorn model,* $P(BM\bar{B}) = 0.5$ – *Popcorn model,* $P(BM\bar{B}) = 1.0$ is easy to conceive, since an increase in the probability of producing an intermediate meson between the $B\bar{B}$ pair results in a deeper and narrower MC correlation between the B and $\bar{B}$ and, on average, also between identical baryons. In the advanced popcorn model, described in [13], the possibility to have more than one intermediate meson is not neglected as in the original popcorn model. However this advanced model predicts a high probability (higher than 0.5) for the B and $\bar{B}$ to be produced as neighbours in rank, whereas the probability for the other configurations $BM^n\bar{B}$ decreases exponentially with n. Any of the current models for baryon production seems to mimic a FD correlation with an associated proton source radius as large as $R \simeq 1\, fm$. Large R values could only be obtained from hypothetical baryon-production models which accounted for high probabilities of production of intermediate mesons, which is not quite expected.

One of the most important possible imperfections in our MC-simulation scheme might be the way the requirements of left-right symmetry and energy-momentum conservation are

Baryon production model	$R\,(fm)$	λ
Diquark model	0.136 ± 0.002	0.781 ± 0.011
Advanced popcorn model [13]	0.140 ± 0.006	0.72 ± 0.03
Popcorn model, $P(BM\bar{B}) = 0.5$	0.150 ± 0.004	0.713 ± 0.014
Popcorn model, $P(BM\bar{B}) = 1.0$	0.161 ± 0.004	0.708 ± 0.015

Table 3: Values of R and λ obtained from equations (33) and (4) for different baryon-production scenarios. In the original popcorn model, $P(BM\bar{B})$ is the probability of producing one meson between a baryon and an antibaryon, while $(1 - P(BM\bar{B}))$ would be the probability of producing the baryon and antibaryon as neighbours in rank.

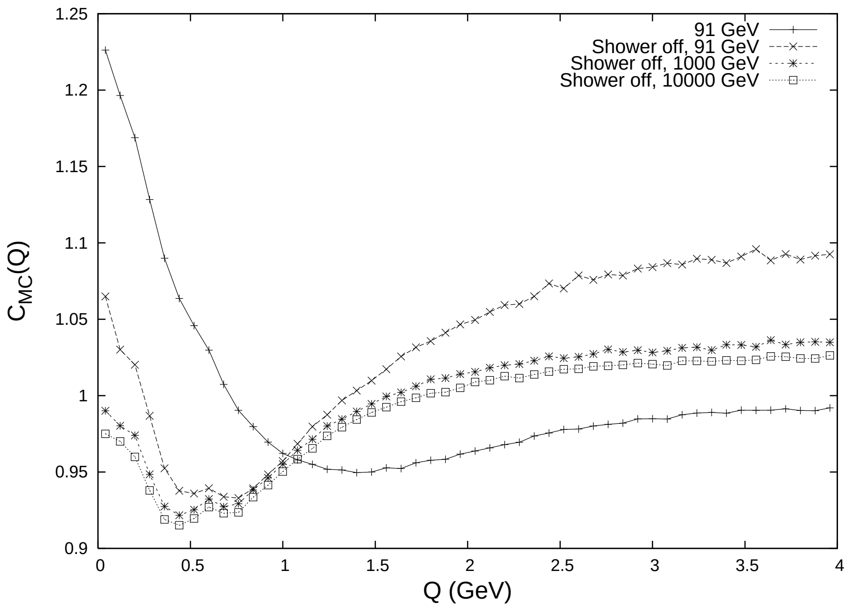

Figure 15: MC correlations for $\pi^+\pi^+$ pairs for different c.m. total energies. "Shower off" indicates that the original quarks are not allowed to branch in the perturbative QCD phase, so that the produced hadrons are emitted only in two jets, along the thrust axis.

ensured in the Lund model. Instead of beginning the iteration of the string fragmentation from the q_0 endpoint all the way to the $\bar{q}_0$ end, or viceversa, each z-step is taken both from the q_0 and the $\bar{q}_0$ end, and the fragmentation is carried until the remaining energy of the system is below approximately $W_{rem} \approx 5\, GeV^2$. Then a final $q\bar{q}$-pair is generated, yielding the last two hadrons. This smooth joining at the centre of the string might give rise to some imperfections in the simulated events. In Fig. 15 we present the MC correlation obtained for charged pions. The unexpected enhancement we find at low Q values may be related to this joining, since it decreases when we increase the total energy, as any possible unpleasant effect arising from the joining should do. It would be interesting to study how the proton FD correlation is affected by changes in the value of the W_{rem} parameter.

5 Summary and conclusions

The two-particle correlation between protons produced in multihadronic events, such as e^-e^+ annihilations, is expected to exhibit a depletion at low momentum separation arising from the Pauli exclusion principle. The shape of this Fermi-Dirac depletion contains information about the space-time characteristics of the region over which the production of the protons occurs. Surprisingly enough, the analyses of recent experimental data have provided a value for the production region size of about $R \approx 0.15\ fm$, which is smaller than the radius of the proton itself. It should be remarked, however, that the Fermi-Dirac correlation function cannot be derived from the raw experimental data only; Monte Carlo generated events are also required in order to determine which part of the experimental distribution of proton momentum separations can be attributed to the antisymmetrization of the two-proton wavefunction. It is therefore natural to consider that some imperfections in the Monte Carlo event simulations might be distorting the results, yielding these unexpectedly small source dimensions.

The Monte Carlo event simulations based on the Lund model depend upon some parameters that cannot be uniquely tuned from observed inclusive particle distributions. It would be interesting to study the uncertainties that these degrees of freedom introduce in the value of the source radius obtained from the data analysis. In this thesis, the qualitative effect of changing the parameters a and b has been investigated. Some MC event simulations have been performed for different values of a and b corresponding to roughly equal average proper time for the breakups, $<\Gamma>\approx (1+a)/b$ (directly related to the event multiplicity), and very similar mixed momentum distributions. We have estimated the shape of the Fermi-Dirac correlations obtained by using these simulated events as different reference samples for the same experimental data. The resulting value for the proton source size R seems to increase for decreasing pairs of values (a, b), in accordance with our expectations. However, this effect is rather small, allowing for a maximum error deviation in the source radius of only $\Delta R/R = 10\%$, approximately. We have to bear in mind that, more precisely, a and b should be changed together with two other parameters, σ and $k_{\perp c}$, for the simulated events to be in good agreement with the experimental inclusive distributions. When one changes the value of $k_{\perp c}$, related to the perturbative QCD phase in an event, the average hadron multiplicity is also modified. In this way, the multiplicity can be kept constant also for different ratios $(1 + a)/b$ if $k_{\perp c}$ is changed appropriately. For this reason, we have also simulated events with random values of a and b corresponding to different average vertex proper times. The source radius obtained by employing these MC simulations can take values from a wider interval, up to around $R \approx 0.25\ fm$; unfortunately, this size is still smaller than the proton radius. Hence, we can conclude that the Fermi-Dirac correlations seem to be only slightly influenced by the chosen values (a, b) of the Monte Carlo simulations that we use as reference samples. More rigorous studies should be made, though, in order to confirm this result. Finally, we have also studied the impact that the choice of the model for baryon production has on the FD correlations. Again, although the resulting value of R varies in the way we had predicted, the range of variation is not large enough to solve the problem.

Given more time, it would be interesting to study the "Monte Carlo correlations" $C_{MC}(Q)$ for some other event-mixing recipes. The shape we obtained for $C_{MC}(Q)$, Fig. 8, is reasonable considering that the protons cannot be produced as neighbours in rank. The DELPHI collaboration apparently has found a mixing procedure that returns a flat MC correlation, $C_{MC}(Q) = 1$. This means that their mixed-event reference sample does not need to be corrected by the double ratio of eq. (6). Hence, they have found an extraordinary mixing technique that conserves all kinds of correlations between protons except for their Fermi-Dirac interference. We must note that the DELPHI collaboration is not performing

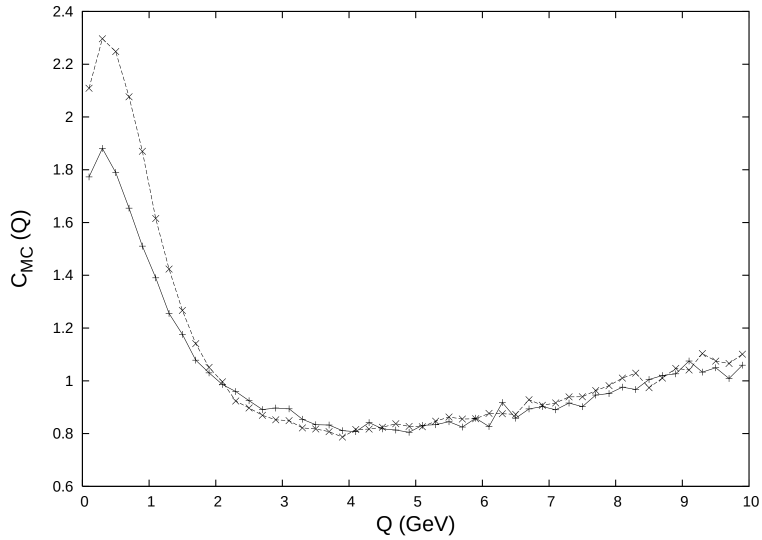

Figure 16: Monte Carlo proton correlation we find in the laboratory frame, without making the thrust axes of different events to coincide. The correlation in broken lines was obtained with the Monte Carlo parameters used by the DELPHI collaboration [20] and the same cut in momenta they impose, accepting only protons with $p > 0.7GeV$.

any thrust analyses of the events.[5] Instead, the differences in momenta are calculated in the laboratory reference frame, without reorienting the events with respect to each other. In this way, protons from different events will show, on average, larger momentum separations than protons produced in the same event. It is then understandable that the Monte Carlo correlation obtained in the laboratory frame will show an increase at low momentum separation Q as compared to the MC correlation derived in the thrust frame. For our mixing technique, however, this increase will not give rise to a flat curve but, rather, to a large enhancement at low Q values, as shown in figure 16. An effort should be made in order to understand the disagreement between DELPHI's and our results.

In summary we have studied some of the uncertainties present in analyses of Fermi-Dirac correlations between pp (and $\Lambda\Lambda$) pairs in e^+e^--annihilations. The effects studied here are significant, but not large enough to fully explain the unexpected results in experimental analyses. The conclusion is therefore that further studies are needed to reveal the true nature of the Fermi-Dirac correlation. This includes in particular the effect of the "junction" between the two halves of the string fragmentation, the effect of experimental cuts, and a combined tuning of the Monte Carlo parameters to both inclusive and correlation data.

[5] In the first paper of reference [10] they mention that the momentum vectors of all proton and antiproton candidates coming from two-proton events are transformed to the reference frame defined by the thrust axis. This statement was apparently a misprint, since in the second paper cited in [10] they do not refer to the thrust axis and the same results are still obtained.

6 Acknowledgements

My deepest gratitude to Gösta Gustafson and Leif Lönnblad for their generous, excellent guidance. I would also like to thank Jake for his kind support, Niclas for our amusing dancing and chess meetings and the rest of the department for making me feel at home.

References

[1] D.H. Boal, C.-K. Gelbke, B.K. Jennings, Rev. Mod. Phys. 62 (1990) 553.

[2] R. Hanbury-Brown, R.Q. Twiss, Nature 178 (1956) 1046.

[3] G. Goldhaber, S. Goldhaber, W. Lee, A. Pais, Phys. Rev. 120 (1960) 300

[4] M. Gyulassy, S.K. Kauffman, L.W. Wilson, Phys. Rev. C20 (1979) 2267.

[5] G. Alexander et al. (OPAL Coll.), Phys. Lett. B384 (1996) 377.

[6] T. Lesiak and H. Palka (DELPHI Coll.), CERN-EP/98-114, DELPHI-CONF-176 (1998)

[7] R. Barate et al. (ALEPH Coll.), Phys. Lett. B475 (2000) 395.

[8] OPAL Coll., CERN-EP/2001, OPAL-PN486 (2001).

[9] R. Barate et al., (ALEPH Coll.), Phys. Lett. B611 (2005) 66-80

[10] DELPHI Coll., DELPHI 2004-038 CONF-713 (23 June, 2004), DELPHI 2005-010 CONF-730 (30 May, 2005).

[11] G. Alexander, Rept. Prog. Phys. 66 (2003) 481-522.

[12] T. Sjöstrand, P. Edén, C. Friberg, L. Lönnblad, G. Miu, S. Mrenna and E. Norrbin, Computer Physics Commun. 135 (2001) 238.

[13] P. Edén and G. Gustafson, Zeitschrift für Physik C75 (1997) 41

[14] R. M. Weiner, Phys. Rept. (2000) 327-249

[15] M. G. Bowler, Z. Phys. C29 (1985) 617

[16] B. Andersson, "The Lund Model", Cambridge University Press (1998)

[17] B. Andersson, G. Gustafson, G. Ingelman, T. Sjöstrand, Phys. Rep. 97 (1983) 31

[18] B. Andersson, G. Gustafson, A. Nilsson, C. Sjögren, Z. Physik C49 (1991) 79

[19] L. Lönnblad, T. Sjöstrand, Eur. Phys. J. C2 (1998) 165-180

[20] P. Abreu et al., (DELPHI Coll.), Z. Phys. C73 (1996) 11